

LETTER TO THE EDITOR

Physical properties of outflows[★]

Comparing CO and H₂O based parameters in Class 0 sources

Bjerkeli, P.¹, Liseau, R.¹, Nisini, B.², Tafalla, M.³, Bergman, P.⁴, Melnick, G.⁵, and Rydbeck, G.¹

¹ Department of Earth and Space Sciences, Chalmers University of Technology, Onsala Space Observatory, 439 92 Onsala, Sweden
e-mail: per.bjerkeli@chalmers.se

² INAF - Osservatorio Astronomico di Roma, Via di Frascati 33, 00040 Monte Porzio Catone, Italy

³ Observatorio Astronómico Nacional (IGN), Calle Alfonso XII,3. 28014, Madrid, Spain

⁴ Onsala Space Observatory, Chalmers University of Technology, 439 92 Onsala, Sweden

⁵ Harvard-Smithsonian Center for Astrophysics, 60 Garden Street, Cambridge, MA 02138, USA

Received 30 January 2013 / Accepted 7 March 2013

ABSTRACT

Context. The observed physical properties of outflows from low-mass sources put constraints on possible ejection mechanisms. Historically, these quantities have been derived from CO observations using ground-based observations. It is thus important to investigate whether parameters such as momentum rate (thrust) and mechanical luminosity (power) are the same when different molecular tracers are used.

Aims. We aim at determining the outflow momentum, dynamical time-scale, thrust, energy and power using CO and H₂O as tracers of outflow activity.

Methods. Within the framework of the WISH key program, three molecular outflows from Class 0 sources have been mapped using the HIFI instrument aboard *Herschel*. We use these observations together with previously published H₂ data to infer the physical properties of the outflows. We compare the physical properties derived here with previous estimates based on CO observations.

Results. Inspection of the spatial distribution of H₂O and H₂ confirms that these molecules are co-spatial. The most prominent emission peaks in H₂ coincide with strong H₂O emission peaks and the estimated widths of the flows when using the two tracers are comparable.

Conclusions. For the momentum rate and the mechanical luminosity, inferred values are independent of which tracer that is used, i.e., the values agree to within a factor of 4 and 3 respectively.

Key words. ISM: individual objects: VLA 1623, L 1448, L 1157 – ISM: molecules – ISM: jets and outflows – stars: formation – stars: winds, outflows

1. Introduction

The emission from CO is a widely used tracer of outflow activity. The lowest rotational transitions emit photons in the millimetre and sub-millimetre part of the electromagnetic spectrum making CO relatively straightforward to observe using ground-based telescopes. Combined with the fact that CO is abundant with respect to molecular hydrogen, this has led to extensive mapping campaigns, covering entire outflows, during the last two decades. Rotational transitions of H₂O and H₂ are, on the contrary, not easily observed from the ground and recent observations have primarily relied on the use of space-based telescopes (e.g. ISO, SWAS and Odin). However, the limited achievable spatial resolution on these missions hampered the possibility to interpret the data. The situation has improved since the launch of *Spitzer* (Werner et al. 2004) and *Herschel* (Pilbratt et al. 2010). It is now possible to observe shocked gas, where the water abundance is expected to be enhanced (see e.g. Bergin et al. 1998; Kaufman & Neufeld 1996), at a much higher spatial resolution.

Some of the physical properties that can be determined from these observations are of fundamental importance in the understanding of the star formation process. For example, the observed ratio between the momentum inputs of outflows and the luminosities of the central sources sets constraints on the possible ejection mechanisms (Lada 1985). Using CO as a tracer, various parameters of interest have therefore been deduced for several molecular outflows in the past (see e.g. André et al. 1990; Bachiller et al. 1990, 2001). It should be noted, however, that uncertainties in the outflow mass and line-of-sight inclination angle can introduce large errors when estimating the total energy and momentum of the outflowing material.

Within the framework of the *Water In Star-forming regions with Herschel* (WISH, van Dishoeck et al. 2011) key program, three nearby molecular outflows from Class 0 sources were observed using the HIFI (de Graauw et al. 2010; Roelfsema et al. 2012) instrument aboard *Herschel*. The mapping observations cover the outflows L1157 (Umemoto et al. 1992), L1448 (Bachiller et al. 1990) and VLA 1623 (André et al. 1990, 1993). Observations of the ground-state transition of *ortho*-water, H₂O(1₁₀ – 1₀₁), at 557 GHz have been discussed, in conjunction with PACS (Poglitsch et al. 2010) observations of the H₂O(2₁₂ – 1₀₁) line at 1670 GHz in

[★] *Herschel* is an ESA space observatory with science instruments provided by European-led Principal Investigator consortia and with important participation from NASA.

Table 1. Observations carried out with HIFI.

Target	α_{2000} (hr:min:s)	δ_{2000} (deg:min:s)	t_{int} (sec)	Obs. ID
L 1448 ^a	03:25:38.40	+30:44:06.0	6468	1342203200
VLA 1623 ^b	16:26:26.38	-24:24:31.0	6552	1342204010
L 1157	20:39:06.20	+68:02:16.0	6440	1342210068

Notes. ^(a)Nisini et al. (2013) ^(b)Bjerkeli et al. (2012)

a series of papers (Nisini et al. 2013; Tafalla et al. 2013; Bjerkeli et al. 2012; Santangelo et al. 2012; Vasta et al. 2012). These outflows were also observed with *Spitzer* and discussed in Neufeld et al. (2009), Nisini et al. (2010b), Giannini et al. (2011) and Bjerkeli et al. (2012). The analysis of the H₂ and H₂O emission suggests that H₂O correlates to a larger extent with H₂ than with low-*J* CO, both in terms of spatial distribution and excitation conditions. The latter molecule is primarily a tracer of the cold, entrained ambient gas while H₂ and H₂O are probing the shocked gas at elevated temperatures (Tafalla et al. 2013; Nisini et al. 2010a; Santangelo et al. 2012). Bjerkeli et al. (2012) compare the physical parameters derived from CO and H₂O for the VLA 1623 outflow. The authors conclude that the force driving the outflow seems to be independent of whether CO or H₂O and H₂ are used as tracers for the outflow. The analysis, however, was based on the observation of a single object and only the north-western outflow lobe of that object. In this letter, we therefore extend this analysis to include also the other outflows that have been mapped with HIFI, i.e. L 1157 and L 1448.

We determine the outflow dynamical age, momentum, momentum rate, energy and mechanical luminosity for L1157, L1448 and VLA 1623. The physical properties derived from the observations of CO(1–0) and CO(2–1) are taken from previously published work. Using the combined spatial and kinematical information obtained from the observations of H₂O and H₂ we then do the same analysis and compare the results.

2. Observations

The *Spitzer* observations of the purely rotational H₂ transitions, H₂ 0 – 0 S(0) to S(7) were originally presented in Neufeld et al. (2009) and we refer the interested reader to that publication.

The mapping observations of the H₂O(1₁₀ – 1₀₁) emission, from the outflows targeted during the WISH program, have already been published (Nisini et al. 2013; Bjerkeli et al. 2012) in recent papers, with one exception, viz. L1157. All three maps were obtained with the HIFI instrument using the “On-The-Fly (OTF) Maps with Position-Switch Reference” observing mode. The maps cover the 5′ by 2′ regions closest to the central source of the outflows, which means that a large proportion of the L 1448 and L 1157 outflows are covered. In the case of VLA 1623, only a small part of the southeastern flow is covered by the observations and consequently we exclude this outflow lobe in the analysis. The data were obtained from the Herschel Science Archive (HSA, v8.2.1 of the pipeline) and standard data reduction methods such as baseline removal and production of maps were done in XS and Matlab. The uncertainty attributed to the calibration is estimated to be ~10% (Roelfsema et al. 2012) and the main beam efficiency at 557 GHz is 0.76 (Olberg 2010). The *Herschel* observations discussed in the present letter are summarised in Table 1 where the corresponding observation identification numbers are listed.

3. Results

For the work presented here, we rely on an estimate of the outflow width and length (when estimating the mass and the dynamical timescale) as measured from the H₂O emission, which is why the HPBW of 38″ at 557 GHz turns out to be a problem. We therefore use a Statistical Image Deconvolution (SID) technique to improve the spatial resolution of the HIFI data (Rydbeck 2008). The deconvolved HIFI maps are presented and overlaid on the *Spitzer* H₂ emission in Fig. 1. From the deconvolution of the maps, we conclude that the widths of the flows are overestimated when using the original datasets. However, the apparent width of the northern flow in L 1157 does not change by a significant amount when the SID method is used, and this part of the flow is likely broader than the southern part. Apart from this single outflow lobe, the outflow lobes have widths of the order ~20″.

The spatial distributions of the H₂ emission regions are in good agreement with the regions responsible for the H₂O emission. The most prominent peaks in the H₂ emission, from all three outflows, are coincident with strong H₂O peaks. However, we note that the H₂O peaks towards the central sources of L 1448 and VLA 1623 are not accompanied with strong H₂ peaks. In the original H₂O data, we detect a weak red-shifted component in the blue-shifted part of the L 1157 outflow. After deconvolution, this emission stands out and the brightness is significantly enhanced. It will, however, not be discussed further here. Note that the H₂O line profiles presented in Nisini et al. (2013) and Bjerkeli et al. (2012) trace velocity ranges equivalent to those of CO. Hence, H₂O does not seem to be special insofar as it traces gas moving at higher or lower speeds than CO. The maximum detected velocity for both molecules are in close agreement (i.e. within a few km s⁻¹).

4. Discussion

In this section we compare the physical properties derived from CO observations to those derived from the H₂O and H₂ observations. Although a resemblance (both what regards the spatial distribution and the excitation conditions) between H₂O and H₂ is well established at this point, it should be noted that this analysis relies on the assumption that also the kinematics are the same. The physical properties of the CO outflows have been presented in André et al. (1990, VLA 1623), Bachiller et al. (1990, L 1448) and Bachiller et al. (2001, L 1157). The results presented in these papers are, however, corrected here, using the most recent method for determining these quantities. The question of how outflows are accelerated is still a matter of debate. It has been argued, however, that the highly collimated outflows that are seen to emanate from the very youngest objects (i.e. Class 0 sources) are best explained by jet-driven models (see e.g. Masson & Chernin 1993; Arce et al. 2007). We therefore calculate the dynamical time-scale, momentum and kinetic energy (t_d , P and E respectively) in the same manner as suggested by Downes & Cabrit (2007, based on numerical simulations of jet-driven outflows). The inclination angles of the flows with respect to the plane of the sky are assumed to be 21°, 15° and 9° for L 1448, VLA 1623 and L 1157, respectively (Girart & Acord 2001; Davis et al. 1999; Gueth et al. 1996). It should be noted that uncertainties in the inferred inclination angles does not affect our main conclusions since the introduced errors are equivalent for CO and H₂O. The largest relevant contribution to the error budget is instead attributed to the estimated molecular mass M of the outflows. Also, as noted by Downes & Cabrit (2007), to use the intensity-weighted velocity $\langle u \rangle_{\text{lobe}}$ (see e.g.

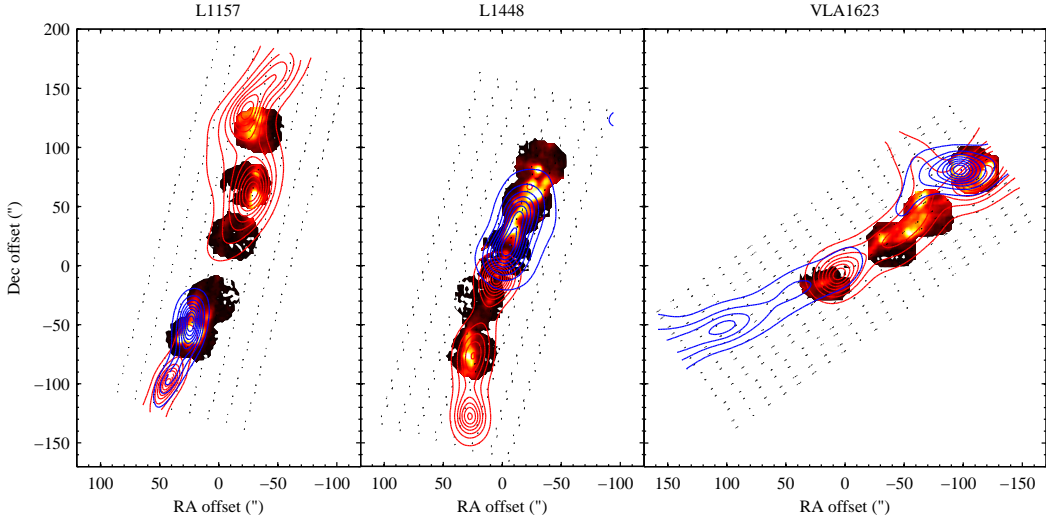


Fig. 1. Colormaps show the sum of the H_2 S(0) - S(7) emission (normalized to $1 \times 10^{-3} \text{ erg cm}^{-2} \text{ s}^{-1} \text{ sr}^{-1}$) and contours of the H_2O ($1_{10} - 1_{01}$) emission are overlaid. Red contours are from 0.06 to 19 K km s^{-1} , 0.09 to 55 K km s^{-1} and 0.05 to 7.9 K km s^{-1} for L 1157, L 1448 and VLA 1623, respectively. Blue contours for the same sources are from 0.06 to 69 K km s^{-1} , 0.09 to 23 K km s^{-1} , and 0.06 to 10 K km s^{-1} . Offsets in the maps are with respect to the central sources, with coordinates tabulated in Table 1. The black dots indicate the readout positions for the OTF maps.

Lada & Fich 1996), averaged over the outflow lobe when determining the dynamical time-scale may overestimate the age of the flow (unless the flow is inclined nearly 90° with respect to the line of sight). Therefore, and as discussed by the same authors, we instead estimate the outflow dynamical ages from the maximum velocity, i.e., dividing the extent of the flow with the maximum inclination corrected velocity $t_d = L_{\text{lobe}}/v_{\text{max}}$. The maximum velocity traced by CO is taken from the literature (André et al. 1990; Bachiller et al. 1990, 2001). When estimating the momentum of the flow we use the intensity-weighted velocity and we do not apply any inclination correction. For the kinetic energy we use a correction factor of 5, i.e., the uncorrected value is multiplied by this number (Downes & Cabrit 2007, their Fig. 4 & 5).

The originally published parameters based on CO data are corrected for most recent distance estimates, 250 pc to L 1157 (Looney et al. 2007), 232 pc to L 1448 (Hirota et al. 2011), and 120 pc to VLA 1623 (Lombardi et al. 2008). The length of the flows are taken to be equal to the maximum extension of the half-power integrated intensity of each lobe. As mentioned earlier, the angular width of all lobes (except the northern flow of L 1157) are close to $20''$. The molecular mass of the H_2O emitting regions is calculated from the estimated H_2 column density (Nisini et al. 2010b; Giannini et al. 2011; Bjerkeli et al. 2012). We assume the typical velocity of the wind to be 200 km s^{-1} , when estimating the mass-loss rate. All inferred quantities are summarised in Table 2.

The highest detected velocity of the H_2O emission line profiles is consistent with previous estimates from CO observations (see Tab. 2). The dynamical ages of the outflows are of the order 10^3 years and this confirms that these sources are very young. They may therefore still be in the formation stage where material is accreted onto the proto-stellar condensation. The dynamical age can be compared to the shock propagation time-scale (the time the gas is in a shocked state) for various types of plane-parallel shock models (Bergin et al. 1998; Flower & Pineau des Forêts 2010). For C-type shocks, time-scales are of the order 10^3 years for a pre-shock density of 10^4 cm^{-3} and even shorter than this for J-type shocks or when

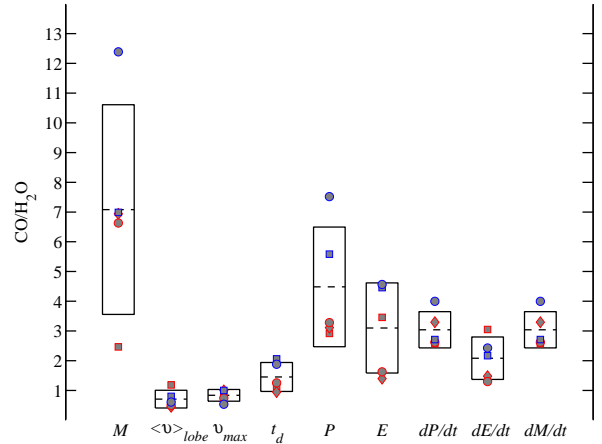


Fig. 2. Ratio between parameters inferred from CO and H_2O observations. The markers indicate the ratios for L 1448 (squares), VLA 1623 (diamonds) and L 1157 (circles). Red and blue colors are for the red and blue outflow lobes, respectively. Note that a few of the symbols are superpositioned. Dashed lines show the mean and boxes indicate the standard deviation.

pre-shock densities are higher. The dynamical ages can therefore be longer than the time-scales for shock propagation. For the outflows discussed here, the water emitting regions trace gas at densities of $\sim 10^6 \text{ cm}^{-3}$ and temperatures higher than 100 K. Under these conditions, the time-scale for freeze-out onto grains should be longer than the dynamical time-scale (Bergin et al. 1998; Hollenbach et al. 2009). Thus, it is possible that once the H_2O abundance is enhanced due to the presence of a shock it will not be significantly reduced in the post-shock region. This is in agreement with the fact that the H_2O emission does not trace gas at particularly high velocities. The thrust dP/dt (momentum rate) and power dE/dt (mechanical luminosity) derived from H_2O and H_2 are in close agreement with previous estimates based on CO observations. However, although the deviations are small, the thrust is on average 3 times higher and the power is 2

Table 2. Physical parameters derived from CO and H₂O observations.

Source:	L1448		VLA 1623		L 1157	
	CO	H ₂ O	CO	H ₂ O	CO	H ₂ O
Molecular tracer:						
<u>Red-shifted lobe</u>						
Total mass (M_{\odot}):	1.6×10^{-2}	6.3×10^{-3}	1.1×10^{-2}	1.6×10^{-3}	8.4×10^{-2}	1.3×10^{-2}
L_{lobe} (pc)	0.17	0.17	0.09	0.09	0.21	0.22
$\langle v \rangle_{\text{lobe}}$ (km s ⁻¹):	75	64	27	60	75	152
v_{max} (km s ⁻¹):	195	218	116	116	143	192
t_{dyn} (yr):	8.7×10^2	7.7×10^2	7.2×10^2	7.6×10^2	1.4×10^3	1.1×10^3
Momentum (M_{\odot} km s ⁻¹):	0.42	0.14	0.08	0.03	0.98	0.30
Kinetic energy (erg):	5.6×10^{44}	1.6×10^{44}	2.7×10^{43}	2.0×10^{43}	5.7×10^{44}	3.5×10^{44}
Momentum rate (M_{\odot} km s ⁻¹ yr ⁻¹):	4.8×10^{-4}	1.9×10^{-4}	1.1×10^{-4}	3.3×10^{-5}	7.0×10^{-4}	2.7×10^{-4}
Mechanical luminosity (L_{\odot}):	5.3×10^0	1.8×10^0	3.1×10^{-1}	2.1×10^{-1}	3.4×10^0	2.6×10^0
Wind mass-loss rate (M_{\odot} yr ⁻¹):	2.4×10^{-6}	9.4×10^{-7}	5.5×10^{-7}	1.7×10^{-7}	3.5×10^{-6}	1.3×10^{-6}
<u>Blue-shifted lobe</u>						
Total mass (M_{\odot}):	2.0×10^{-2}	2.8×10^{-3}			1.2×10^{-1}	9.4×10^{-3}
L_{lobe} (pc)	0.16	0.08			0.12	0.12
$\langle v \rangle_{\text{lobe}}$ (km s ⁻¹):	-75	-94			-29	-49
v_{max} (km s ⁻¹):	-195	-195			-68	-128
t_{dyn} (yr):	7.8×10^2	3.8×10^2			1.8×10^3	9.4×10^2
Momentum (M_{\odot} km s ⁻¹):	0.53	0.09			0.54	0.07
Kinetic energy (erg):	7.1×10^{44}	1.6×10^{44}			1.2×10^{44}	2.7×10^{43}
Momentum rate (M_{\odot} km s ⁻¹ yr ⁻¹):	6.7×10^{-4}	2.5×10^{-4}			3.0×10^{-4}	7.6×10^{-5}
Mechanical luminosity (L_{\odot}):	7.5×10^0	3.4×10^0			5.8×10^{-1}	2.4×10^{-1}
Wind mass-loss rate (M_{\odot} yr ⁻¹):	3.4×10^{-6}	1.2×10^{-6}			1.5×10^{-6}	3.8×10^{-7}

Notes. Inclination angles with respect to the plane of the sky are 21°, 15°, and 9° for L 1448, VLA 1623 and L 1157, respectively. The velocity of the wind is assumed to be 200 km s⁻¹.

times higher when deduced from CO observations (see Fig. 2). The reason for this is not entirely clear but it may be that the mass of the H₂O emitting gas in reality is slightly larger than the values estimated from this work. The wind mass-loss rates are estimated to be $\sim 10^{-6} M_{\odot} \text{ yr}^{-1}$ for L 1448 and L 1157, and one order of magnitude lower for VLA 1623. Assuming that the luminosity of the central source¹ is entirely due to accretion and adopting a radius to mass ratio of 5, this leads to similar values for the mass-accretion rates (see e.g. Stahler et al. 1980).

5. Conclusions

The inferred values for power agrees to within a factor of 3, when using the different molecular tracers. Similarly, the estimated values for thrust are equal to within a factor of 4. This may indicate that the ejection mechanism that is responsible for the motion of the cold gas, is the same as the one that sets the warm gas into motion. It is, however, also possible that this is a characteristic of young outflows. This study also reveals that the emission from H₂O traces a gas component that presumably operates on the same time-scales as CO, i.e. H₂O is not detected at very different velocities compared to CO. The fact that the estimated values are the same (within a factor of a few) for all observed sources supports previous estimates based on CO observations. We also find it likely, that ground-based CO observations are adequate, when assessing the impact of outflows on their environment.

Acknowledgements. P. Bjerkeli wish to thank Eva Wirström for interesting discussions. The authors appreciate the support from the Swedish National Space Board (SNSB). HIFI has been designed and built by a consortium of institutes and university departments from across Europe, Canada and the United States under the leadership of SRON Netherlands Institute

¹ $L_{\text{bol}} = 8.3, 8.4,$ and <2.0 for L 1448, L 1157 and VLA 1623 respectively (Froeblich 2005).

for Space Research, Groningen, The Netherlands and with major contributions from Germany, France and the US. Consortium members are: Canada: CSA, U. Waterloo; France: CESR, LAB, LERMA, IRAM; Germany: KOSMA, MPIfR, MPS; Ireland, NUI Maynooth; Italy: ASI, IFSI-INAF, Osservatorio Astrofisico di Arcetri- INAF; Netherlands: SRON, TUD; Poland: CAMK, CBK; Spain: Observatorio Astronómico Nacional (IGN), Centro de Astrobiología (CSIC-INTA). Sweden: Chalmers University of Technology - MC2, RSS & GARD; Onsala Space Observatory; Swedish National Space Board, Stockholm University - Stockholm Observatory; Switzerland: ETH Zurich, FHNW; USA: Caltech, JPL, NHSC.

References

- André, P., Martín-Pintado, J., Despois, D., & Montmerle, T. 1990, *A&A*, 236, 180
 André, P., Ward-Thompson, D., & Barsony, M. 1993, *ApJ*, 406, 122
 Arce, H. G., Shepherd, D., Gueth, F., et al. 2007, in *Protostars and Planets V*, ed. B. Reipurth, D. Jewitt, & K. Keil, 245–260
 Bachiller, R., Martín-Pintado, J., Tafalla, M., Cernicharo, J., & Lazareff, B. 1990, *A&A*, 231, 174
 Bachiller, R., Pérez Gutiérrez, M., Kumar, M. S. N., & Tafalla, M. 2001, *A&A*, 372, 899
 Bergin, E. A., Neufeld, D. A., & Melnick, G. J. 1998, *ApJ*, 499, 777
 Bjerkeli, P., Liseau, R., Larsson, B., et al. 2012, *A&A*, 546, A29
 Davis, C. J., Smith, M. D., Eislöffel, J., & Davies, J. K. 1999, *MNRAS*, 308, 539
 de Graauw, T., Helmich, F. P., Phillips, T. G., et al. 2010, *A&A*, 518, L6+
 Downes, T. P. & Cabrit, S. 2007, *A&A*, 471, 873
 Flower, D. R. & Pineau des Forêts, G. 2010, *MNRAS*, 406, 1745
 Froeblich, D. 2005, *ApJS*, 156, 169
 Giannini, T., Nisini, B., Neufeld, D., et al. 2011, *ApJ*, 738, 80
 Girart, J. M. & Acord, J. M. P. 2001, *ApJ*, 552, L63
 Gueth, F., Guilloteau, S., & Bachiller, R. 1996, *A&A*, 307, 891
 Hirota, T., Honma, M., Imai, H., et al. 2011, *PASJ*, 63, 1
 Hollenbach, D., Kaufman, M. J., Bergin, E. A., & Melnick, G. J. 2009, *ApJ*, 690, 1497
 Kaufman, M. J. & Neufeld, D. A. 1996, *ApJ*, 456, 611
 Lada, C. J. 1985, *ARA&A*, 23, 267
 Lada, C. J. & Fich, M. 1996, *ApJ*, 459, 638
 Lombardi, M., Lada, C. J., & Alves, J. 2008, *A&A*, 489, 143
 Looney, L. W., Tobin, J. J., & Kwon, W. 2007, *ApJ*, 670, L131
 Masson, C. R. & Chernin, L. M. 1993, *ApJ*, 414, 230

- Neufeld, D. A., Nisini, B., Giannini, T., et al. 2009, *ApJ*, 706, 170
- Nisini, B., Benedettini, M., Codella, C., et al. 2010a, *A&A*, 518, L120+
- Nisini, B., Giannini, T., Neufeld, D. A., et al. 2010b, *ApJ*, 724, 69
- Nisini, B., Santangelo, G., Antonucci, S., et al. 2013, *A&A*, 549, A16
- Olberg, M. 2010, Technical Note: ICC/2010-nnn, v1.1, 2010-11-17
- Pilbratt, G. L., Riedinger, J. R., Passvogel, T., et al. 2010, *A&A*, 518, L1+
- Poglitsch, A., Waelkens, C., Geis, N., et al. 2010, *A&A*, 518, L2+
- Roelfsema, P. R., Helmich, F. P., Teyssier, D., et al. 2012, *A&A*, 537, A17
- Rydbeck, G. 2008, *ApJ*, 675, 1304
- Santangelo, G., Nisini, B., Giannini, T., et al. 2012, *A&A*, 538, A45
- Stahler, S. W., Shu, F. H., & Taam, R. E. 1980, *ApJ*, 241, 637
- Tafalla, M., Liseau, R., Nisini, B., et al. 2013, *ArXiv e-prints*
- Umemoto, T., Iwata, T., Fukui, Y., et al. 1992, *ApJ*, 392, L83
- van Dishoeck, E. F., Kristensen, L. E., Benz, A. O., et al. 2011, *PASP*, 123, 138
- Vasta, M., Codella, C., Lorenzani, A., et al. 2012, *A&A*, 537, A98
- Werner, M. W., Roellig, T. L., Low, F. J., et al. 2004, *ApJS*, 154, 1